



Evaluation of Four Imaging Techniques for the Electrical Characterization of Solar Cells

Preprint

G.M. Berman, N. Call, R.K. Ahrenkiel
and S.W. Johnston

National Renewable Energy Laboratory

*Presented at the 2008 Materials Research Society (MRS)
Fall Meeting
Boston, Massachusetts
November 30 – December 5, 2008*

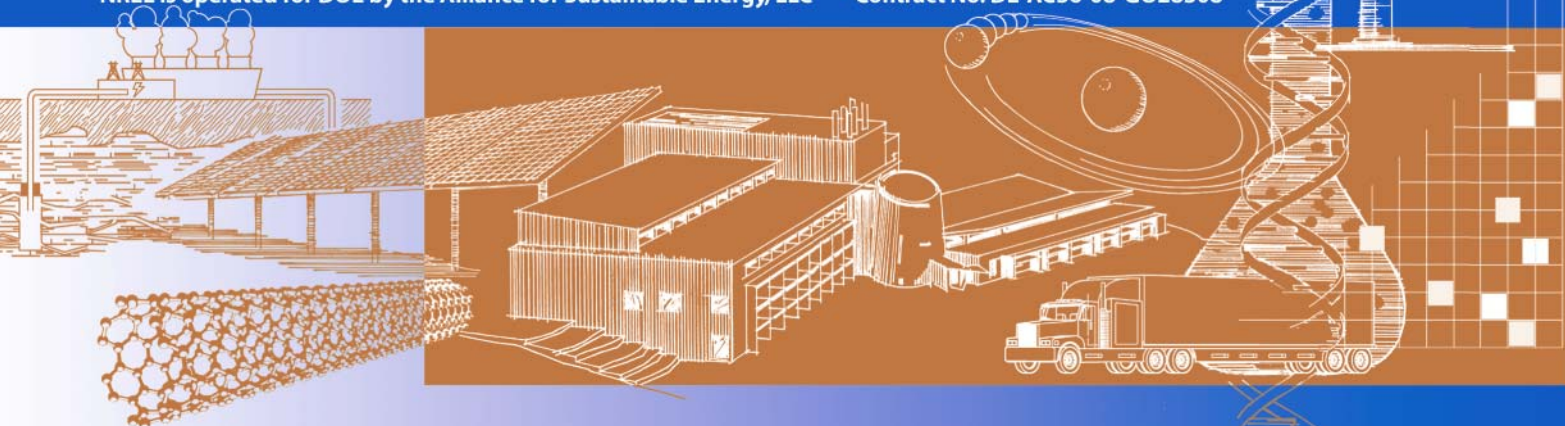
Conference Paper

NREL/CP-520-44607

December 2008

NREL is operated for DOE by the Alliance for Sustainable Energy, LLC

Contract No. DE-AC36-08-GO28308



NOTICE

The submitted manuscript has been offered by an employee of the Alliance for Sustainable Energy, LLC, (ASE) a contractor of the US Government under Contract No. DE-AC36-08GO28308. Accordingly, the US Government and ASE retain a nonexclusive royalty-free license to publish or reproduce the published form of this contribution, or allow others to do so, for US Government purposes.

This report was prepared as an account of work sponsored by an agency of the United States government. Neither the United States government nor any agency thereof, nor any of their employees, makes any warranty, express or implied, or assumes any legal liability or responsibility for the accuracy, completeness, or usefulness of any information, apparatus, product, or process disclosed, or represents that its use would not infringe privately owned rights. Reference herein to any specific commercial product, process, or service by trade name, trademark, manufacturer, or otherwise does not necessarily constitute or imply its endorsement, recommendation, or favoring by the United States government or any agency thereof. The views and opinions of authors expressed herein do not necessarily state or reflect those of the United States government or any agency thereof.

Available electronically at <http://www.osti.gov/bridge>

Available for a processing fee to U.S. Department of Energy
and its contractors, in paper, from:

U.S. Department of Energy
Office of Scientific and Technical Information
P.O. Box 62
Oak Ridge, TN 37831-0062
phone: 865.576.8401
fax: 865.576.5728
email: <mailto:reports@adonis.osti.gov>

Available for sale to the public, in paper, from:

U.S. Department of Commerce
National Technical Information Service
5285 Port Royal Road
Springfield, VA 22161
phone: 800.553.6847
fax: 703.605.6900
email: orders@ntis.fedworld.gov
online ordering: <http://www.ntis.gov/ordering.htm>



Printed on paper containing at least 50% wastepaper, including 20% postconsumer waste

Evaluation of Four Imaging Techniques for the Electrical Characterization of Solar Cells

Gregory M. Berman^{1,3}, Nathan J. Call^{2,3}, Richard K. Ahrenkiel^{2,3}, and Steven W. Johnston³

¹Department of Electrical Engineering, University of Colorado, Boulder, CO 80309, U.S.A.

²Department of Materials Science, Colorado School of Mines, Golden, CO 80401, U.S.A.

³National Renewable Energy Laboratory, Golden, CO 80401, U.S.A.

ABSTRACT

We evaluate four techniques that image minority carrier lifetime, carrier diffusion length, and shunting in solar cells. The techniques include photoluminescence imaging, carrier density imaging, electroluminescence imaging, and dark lock-in thermography shunt detection. We compare these techniques to current industry standards and show how they can yield similar results with higher resolution and in less time.

INTRODUCTION

In this paper, we address four imaging techniques that measure minority carrier lifetime, diffusion length, and the location of shunts in a solar cell, and we compare our techniques to methods currently used in industry. Minority-carrier-lifetime and diffusion-length measurements are critical for characterizing the quality of solar materials to predict the efficiency of a device made from them [1-2]. Shunts can drastically lower a solar cell's efficiency and are introduced in the processing of a wafer into a working solar cell [3].

Minority carrier lifetime is the average time it takes for a free carrier generated in a material to recombine. We measure it with photoluminescence imaging (PLI) and carrier-density imaging (CDI). PLI probes the radiative recombination of an optically excited sample, which is proportional to the sample's carrier density [4-6]. CDI measures the transmission of infrared (IR) light through an optically excited sample, which is also proportional to carrier density [7-8]. We compare these two carrier-lifetime techniques to each other and to microwave-reflection photoconductive decay on a Semilab tool, an industry standard that relates a material's conductivity to its carrier density.

Carrier diffusion length is the average distance a free carrier travels in a material before it recombines. We measure it with electroluminescence imaging (ELI). ELI probes the radiative recombination of a finished solar cell that is electrically driven in forward bias [9-10]. We compare ELI images with light-beam-induced current (LBIC) maps [11], an industry standard that measures the optically induced current in a solar cell.

Shunts are defects created during solar cell processing that leak current. We use dark lock-in thermography (DLIT) to detect them. While shunts can be detected by measuring a cell's I-V (current-voltage) curve, no information about a shunt's cause or location is identified. In DLIT imaging, the solar cell is put under reverse bias, and the shunts are detected by a thermal signature, generated by current leaking across the p-n junction [12]. We demonstrate shunt detection and identify the defect with a scanning electron microscope.

METHODS

Photoluminescence imaging

PLI is the steady-state equivalent of time-resolved photoluminescence that is imaged onto a camera. This technique has recently been made possible by the high sensitivity and large pixel counts of modern Si charge-coupled-device (CCD) cameras. During PLI, carriers in a wafer or a finished cell are optically excited. The camera then detects a small amount of radiative recombination from the indirect bandgap material. Areas on the sample that have long minority-carrier lifetimes will have a higher steady-state density of free carriers, resulting in a stronger radiative recombination signal.

We collect PLI data using a PIXIS 1024BR Si CCD camera (Princeton Instruments/Acton). This camera has a 1024 x 1024 array of 13 μm pixels and is back illuminated and cooled to 200 K. The detector is deep depleted to enhance quantum efficiency beyond 1100 nm. A compact lens (Schneider Optics Cinegon) is mounted to the camera along with a stack of two 810 nm notch filters (Kaiser Optical Systems). A black glass filter (Schott RG1000) is placed between the two notch filters to eliminate resonance. The filter stack is designed to sufficiently attenuate reflected light from the 60 W, 810 nm laser diode excitation source. The fiber output from the laser diode is expanded to the sample area by a collimator and an engineered diffuser.

Measurements are made while the sample is under steady-state illumination. The image is a summation of all photons collected in a set exposure time. It is a spatial map of the radiative recombination in the sample, which is directly related to carrier concentration and carrier lifetime. While such images are qualitative, we show that they can be calibrated by transient-lifetime measurements to yield absolute lifetime values.

Carrier density imaging

CDI is a direct measurement of free carriers in a process called free-carrier absorption. Free-carrier absorption occurs when excited carriers decrease the transmission of mid-to-far infrared light in a semiconductor. During this process, a wafer without any metallization is optically excited. Then an infrared camera images the change in transmission of black-body radiation through a sample with and without the excited carriers.

CDI data is acquired with a Silver 660M InSb infrared camera (ElectroPhysics/Cedip), which has a 640 x 512 array of 15 μm pixels and a spectral response from 3.6–5.1 μm . A built-in Stirling stage cools the detector to ~ 76 K. The camera has a built-in lock-in feature and a maximum frame rate of 100 Hz. We use the camera's lock-in mode to collect CDI data with the laser diode driven by a 27 Hz square wave. The lock-in mode greatly reduces the noise of the measurements — a critical factor for measuring the small signals in CDI. We used a hot plate set at ~ 400 K as the black-body source. To enhance the hotplate's emissivity, we have coated it with a black high-temperature paint.

The images we collect represent the amplitude of the Fourier transform of each pixel in time at the particular frequency we are collecting data. The images show the relative change in transmission spatially across the wafer. This transmission is proportional to the lifetime. While these images are qualitative by themselves, they can be calibrated by a single-point lifetime measurement to yield accurate lifetime images.

Electroluminescence imaging

We collect ELI data in much the same way as PLI. We use the same Si CCD camera, though we take off the filter stacks since there is no laser excitation light to filter out. Others have used various filter arrangements to enhance ELI data and analysis [10]. In ELI, a finished solar cell is electrically driven in forward bias like a light emitting diode. As in PLI, the measurement is taken under steady-state excitation with a typical exposure time of one second. Raw ELI data is qualitative, but can be made quantitative by the method of data collection and analysis [9].

Dark lock-in thermography

To detect shunts using DLIT imaging, a finished wafer is electrically driven in reverse bias. The reverse bias is applied to the sample by an amplifier driven by a square wave. An ideal solar cell under reverse bias would have very little current flow. However, imperfections in the cell often lead to areas where there is a lower virtual resistance through the cell's junction, causing current to flow through it. This flow of current then generates heat, creating hotspots that we image in lock-in mode with the same thermal camera used in CDI.

RESULTS AND DISCUSSION

Comparison of PLI and CDI to transient lifetime measurements

Our data show that there is a strong correlation between PLI and CDI as well as with the actual measured lifetime on a wafer. For the absolute measurement, we use the microwave-reflection-photoconductive-decay technique built into a Semilab lifetime-measurement tool. This technique measures the conductivity of a material, which is proportional to the carrier density, by detecting the change in reflection of microwaves off the sample. The lifetime is then found from the carrier-concentration decay rate after a laser pulse illuminates the sample. It then takes ~6 minutes to map a 5-inch standard wafer at a resolution of 1 mm. Resolution is limited to the excitation light cross-section incident on the sample. A PLI image of the same wafer is collected in ~1 second at a resolution of ~125 μm . Likewise, a CDI image is made in ~10 seconds with a resolution of ~250 μm . The resolution is ultimately limited by the diffraction limit of light, which is ~1 μm for PLI and ~5 μm for CDI. The disadvantage of these imaging techniques is that they do not yield quantitative results. The lack of quantitative results is shown in Fig. 1, where only the Semilab map has a scale for the lifetime.

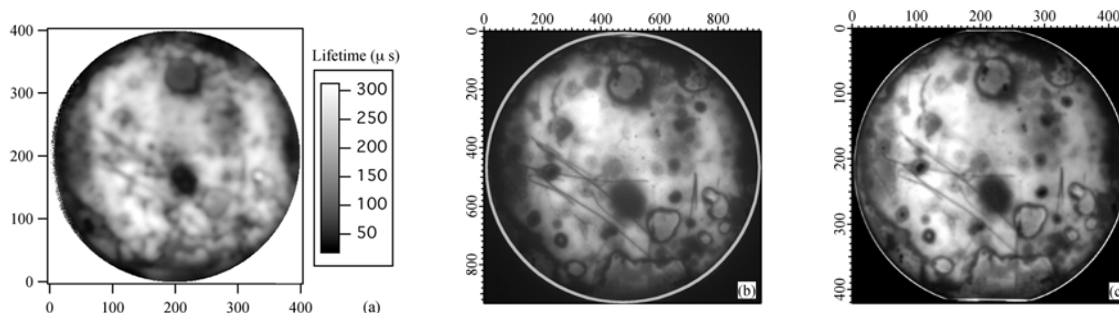
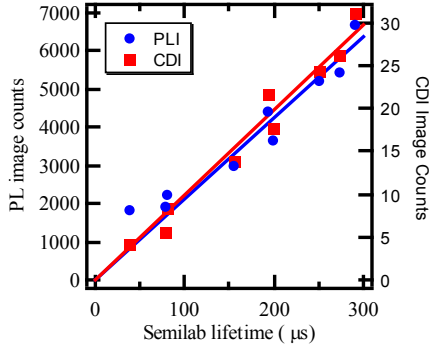


Figure 1. Lifetime of CZ Si wafer with induced impurities acquired from (a) a Semilab lifetime scanner, (b) photoluminescence imaging, and (c) carrier-density imaging.



To obtain a quantitative analysis of the imaging techniques, we compare identical points on a wafer with each technique and plot them against each other. We find that there is a linear relationship between the pixel counts, the signal strength at a single pixel, and the measured lifetime values on the Semilab tool. By measuring two different points on a wafer with the Semilab tool, we can create a calibration constant to transform both PLI and CDI data into quantitative lifetime values, as shown in Fig. 2.

Figure 2. Comparison of PLI and CDI data with Semilab lifetime measurements at discrete points on a CZ Si wafer to calibrate image values to absolute lifetime.

Comparison of ELI to LBIC diffusion-length measurements

The standard method of mapping carrier-diffusion length in a finished cell is through the LBIC technique. Mapping a 5-inch square wafer takes ~6 hours at a resolution of 250 μm , as seen in Fig. 3(a) and (b). For the same wafer, ELI images can be collected in ~1 second at a resolution of ~125 μm , as seen in Fig. 4(a) and (b). Although the correlation between the LBIC measurement and ELI may not appear linear, Fig. 3(c) and 4(c) illustrate the similarity between them. Such correlations have been quantified in detail previously [9].

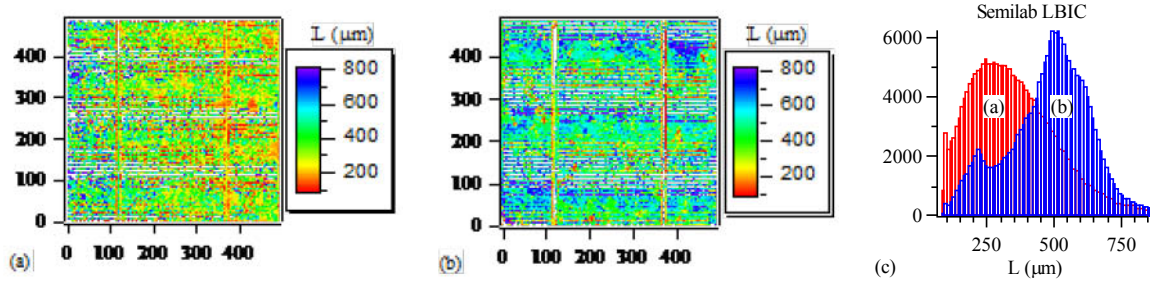


Figure 3. LBIC carrier-diffusion-length map for (a) a low-efficiency wafer and (b) a high-efficiency wafer. (c) Comparative histogram of the diffusion lengths of (a) and (b).

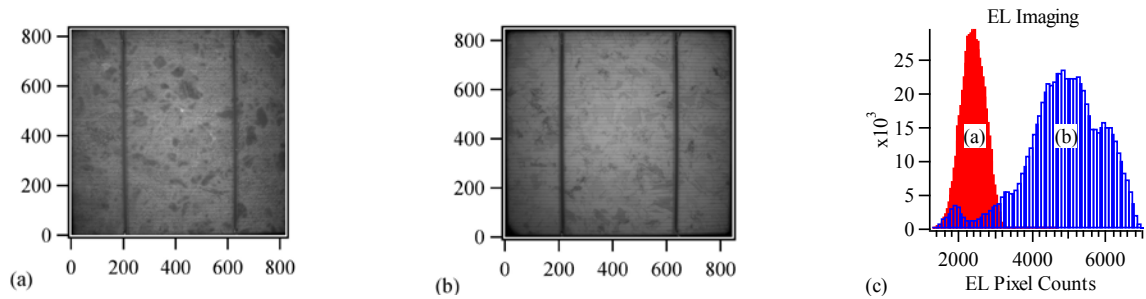


Figure 4. Electroluminescence imaging of the relative carrier-diffusion length for (a) a low-efficiency wafer and (b) a high-efficiency wafer. (c) Comparative histograms of the image pixel counts of (a) and (b).

Shunt Detection and Analysis using DLIT

Using DLIT, we can find the location of all the major shunts on a wafer and gain insight into their cause as shown in Fig. 5. We can determine which shunts are leaking the most current from the amplitude image [Fig. 5(b)]. In the phase image [Fig. 5(c)], we can see how fast heat is spreading from different points in the sample, which allows us to resolve smaller shunts.

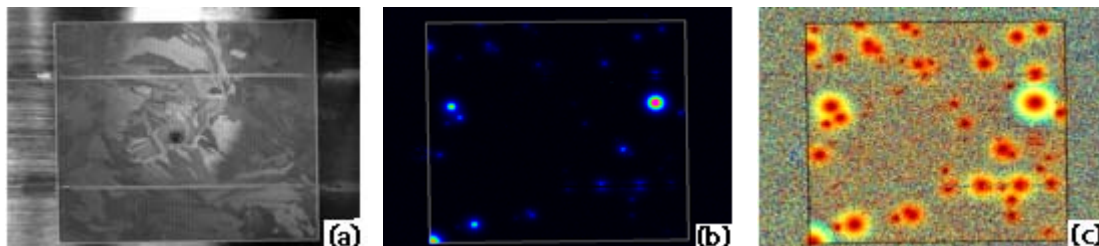


Figure 5. Thermographic shunt detection in a multicrystalline Si wafer at 4 V reverse bias. (a) Thermal image. (b) Lock-in amplitude image. (c) Lock-in phase image. Units are arbitrary.

To get a better understanding of what may be causing shunts, we use a microscopic objective on our thermal camera to view specific shunts at a higher optical resolution. Often a shunt can be seen on a gridline where the metallization has punctured through the emitter layer. In some cases, a bright shunt in the shape of a line corresponds to a crack in the wafer that was filled in during metallization, causing a catastrophic shunt that ruins the device. For the case shown in Fig. 6, an aluminum particle has punctured through the emitter layer, creating a path for current to flow. In the zoomed-in DLIT image, the shunt seems asymmetric. A scanning electron microscope image [Fig. 6(b)] shows that this asymmetric shunt corresponds to an embedded aluminum particle.

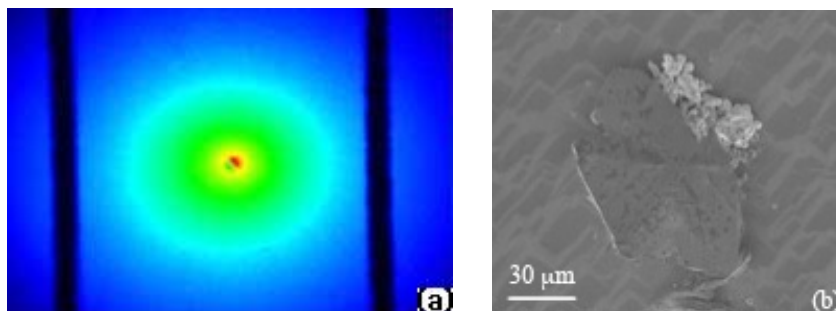


Figure 6. Images of a shunt caused by an embedded aluminum particle using (a) a thermal camera in lock-in mode with $\sim 50\times$ magnification and (b) a scanning electron microscope.

CONCLUSIONS

We have demonstrated imaging methods for minority carrier lifetime (PLI, CDI) and diffusion length (ELI) that give much faster and higher resolution data than traditional single-point mapping techniques. For carrier lifetime imaging, we have shown that a single-point calibration can easily transform a qualitative image into actual lifetime values. These imaging techniques enable the possibility of higher-level quality control and defect analysis of solar cell materials in in-line production processes.

We have used DLIT to find the location of shunts on a wafer and trace them back to specific points in the production process. In industry, this information could be used to address problems in production and increase the yield of working wafers with higher efficiencies.

ACKNOWLEDGMENTS

We thank CaliSolar Inc. for providing solar cells, Dr. Jian Li and Mr. Jerry Tynan for their assistance in the experimental set-up, Mr. Bobby To for taking the SEM images, and Dr. Mowafak Al-Jassim and Dr. Dean Levi for coordinating this work. This work was supported by the U.S. Department of Energy under Contract No. DE-AC36-08GO28308 with the National Renewable Energy Laboratory (NREL) and under NREL's Solar America Initiative PV Incubator program.

REFERENCES

1. D. K. Schroder, *Semiconductor Material and Device Characterization*, (John Wiley & Sons, Inc., New York, 1990).
2. J. W. Orton and P. Blood, *The Electrical Characterization of Semiconductors: Measurement of Minority Carrier Properties* (Academic Press, Inc., San Diego, CA 1990).
3. O. Breitenstein and M. Langenkamp, *Lock-in Thermography – Basics and Uses for Functional Diagnostics of Electrical Components* (Springer, New York, 2003).
4. Y. Koshka, S. Ostapenko, I. Tarasov, S. McHugo, and J. P. Kalejs, *Appl. Phys. Lett.* **74**, 1555 (1999).
5. M. Tajima, Z. Li, S. Sumie, H. Hashizume, and A. Ogura, *Jpn. J. Appl. Phys.* **43**, 432 (2004).
6. T. Trupke, R. A. Bardos, M. C. Schubert, and W. Warta, *Appl. Phys. Lett.* **89**, 044107 (2006).
7. M. Bail, J. Kentsch, R. Brendel, and M. Schulz, *Proceedings of the 28th IEEE-PVSC*, Anchorage, AK, 99 (2000).
8. J. Isenberg, S. Riepe, S. W. Glunz, and W. Warta, *J. Appl. Phys.* **93**, 4268 (2003).
9. T. Fuyuki, H. Kondo, T. Yamazaki, Y. Takahashi, and Y. Uraoka, *Appl. Phys. Lett.* **86**, 262108 (2005).
10. P. Wurfel, T. Trupke, M. Rudiger, T. Puzzer, E. Schaffer, W. Warta, and S. W. Glunz, *22nd European Photovoltaic Solar Energy Conference and Exhibition*, Milan, Italy (2007).
11. O. Palais, J. Gervais, E. Yakimov, and S. Martinuzzi, *Eur. Phys. J. AP* **10**, 157 (2000).
12. O. Breitenstein in *17th Workshop on Crystalline Silicon Solar Cells and Modules: Materials and Processes*, edited by B. L. Sopori (2007).

REPORT DOCUMENTATION PAGE

Form Approved
OMB No. 0704-0188

The public reporting burden for this collection of information is estimated to average 1 hour per response, including the time for reviewing instructions, searching existing data sources, gathering and maintaining the data needed, and completing and reviewing the collection of information. Send comments regarding this burden estimate or any other aspect of this collection of information, including suggestions for reducing the burden, to Department of Defense, Executive Services and Communications Directorate (0704-0188). Respondents should be aware that notwithstanding any other provision of law, no person shall be subject to any penalty for failing to comply with a collection of information if it does not display a currently valid OMB control number.

PLEASE DO NOT RETURN YOUR FORM TO THE ABOVE ORGANIZATION.

1. REPORT DATE (DD-MM-YYYY) December 2008			2. REPORT TYPE Conference Paper		3. DATES COVERED (From - To)	
4. TITLE AND SUBTITLE Evaluation of Four Imaging Techniques for the Electrical Characterization of Solar Cells:Preprint				5a. CONTRACT NUMBER DE-AC36-08-GO28308		
				5b. GRANT NUMBER		
				5c. PROGRAM ELEMENT NUMBER		
6. AUTHOR(S) G.M. Berman, N.J. Call, R.K. Ahrenkiel, and S.W. Johnston				5d. PROJECT NUMBER NREL/CP-520-44607		
				5e. TASK NUMBER PVA93110		
				5f. WORK UNIT NUMBER		
7. PERFORMING ORGANIZATION NAME(S) AND ADDRESS(ES) National Renewable Energy Laboratory 1617 Cole Blvd. Golden, CO 80401-3393				8. PERFORMING ORGANIZATION REPORT NUMBER NREL/CP-520-44607		
9. SPONSORING/MONITORING AGENCY NAME(S) AND ADDRESS(ES)				10. SPONSOR/MONITOR'S ACRONYM(S) NREL		
				11. SPONSORING/MONITORING AGENCY REPORT NUMBER		
12. DISTRIBUTION AVAILABILITY STATEMENT National Technical Information Service U.S. Department of Commerce 5285 Port Royal Road Springfield, VA 22161						
13. SUPPLEMENTARY NOTES						
14. ABSTRACT (Maximum 200 Words) We evaluate four techniques that image minority-carrier lifetime, carrier diffusion length, and shunting in solar cells. The techniques include photoluminescence imaging, carrier-density imaging, electroluminescence imaging, and dark lock-in thermography shunt detection. We compare these techniques to current industry standards and show how they can yield similar results with higher resolution and in less time.						
15. SUBJECT TERMS PV; imaging techniques; minority-carrier lifetime; carrier diffusion length; shunting; solar cells; photoluminescence imaging; carrier-density imaging; electroluminescence imaging; dark lock-in thermography shunt detection;industry standards;						
16. SECURITY CLASSIFICATION OF:			17. LIMITATION OF ABSTRACT UL	18. NUMBER OF PAGES	19a. NAME OF RESPONSIBLE PERSON	
a. REPORT Unclassified	b. ABSTRACT Unclassified	c. THIS PAGE Unclassified			19b. TELEPHONE NUMBER (Include area code)	

Standard Form 298 (Rev. 8/98)
Prescribed by ANSI Std. Z39.18